GUST GENERATOR FOR
A SUPERSONIC WIND TUNNEL

Bobby W. Sanders, Allan R. Bishop,
and John A. Webb, Jr.

Lewis Research Center
Cleveland, Ohio 44135

GUST GENERATOR FOR A SUPERSONIC WIND TUNNEL

by Bobby W. Sanders, Allan R. Bishop,
and John A. Webb, Jr.

Lewis Research Center

SUMMARY

An investigation was conducted to determine the effectiveness of a flat plate gust generator that was located in the nozzle throat of the Lewis 10- by 10-Foot Supersonic Wind Tunnel. Gust plates were tested at three Mach numbers that are representative of the Mach number range of the wind tunnel. The effect of plate height, vertical location of the plate above the floor, and Reynolds number were investigated.

The majority of the data were obtained with the plates fixed in the vertical (maximum blockage) position. In practice Mach number variations would be provided by rotating the plate about its axis. One transient data point in which the plate, hinged at the bottom, was allowed to rotate from the vertical position $\left(\text{local free stream Mach number } M_l = 2.57\right)$ to a horizontal position $\left(\text{minimum blockage position, } M_l = 2.42\right)$ was recorded. These data show that a gust can be provided in the tunnel test section by using a flat plate gust generator in the nozzle throat. In addition to a change in test section free stream Mach number, a variation in airflow angle and total pressure occurred. Data that were recorded for the three test wall Mach numbers of 3.1, 2.4, and 2.0 indicate that a test model must be mounted at a location in the test section where the desired initial Mach number was present and where oblique shocks are not present. A gust amplitude of 0.15 in test section Mach number was provided by rotating a gust plate in the throat. Data show that variations in test section Mach number greater than 0.10 can be provided at all of the test Mach numbers.

Analysis of the dynamic data point shows a corner frequency of at least 8 hertz.

INTRODUCTION

Steady-state and internal airflow transient data have been obtained for numerous inlets and inlet-engine combinations in wind tunnels. However, additional investigation is required to more completely define the capabilities of these propulsion systems to withstand transients in external airflow. In general, the tolerances of the propulsion systems to external airflow disturbances have not fully been investigated because the

available test facilities do not have the required capability of simulating large amplitude gust conditions.

Free stream gust conditions that are encountered by a supersonic aircraft have been simulated in the Lewis 10- by 10-Foot Supersonic Wind Tunnel by oscillating a large plate that was positioned just upstream of an inlet model (refs. 1 to 3). Due to the force and power requirements that were necessary to oscillate the large gust plate, large gust amplitudes have only been obtained at gust frequencies below 15 hertz. Drive power requirements for gust generators of this type for larger inlet models than the 63.5-centimeter (25-in.) inlets of references 1 to 3 is prohibitive since the size of the plate must be increased as the model size is increased. Large gust plates in addition to a large test model can also cause tunnel starting problems. Reference 4 indicates that a similar system has been used to simulate an atmospheric gust in the Ames 8- by 7-Foot Supersonic Wind Tunnel.

The objective of this study was to evaluate the effectiveness of a potential gust generator concept for the Lewis 10- by 10-Foot Supersonic Wind Tunnel. Basically, the gust generator was obtained by installing a flat plate in the nozzle of the tunnel. In concept, the free stream gust would be provided by rotating this flat plate or a paddle wheel arrangement about its axis. This rotation of the plate would provide variations in nozzle throat area which would result in changes in test section free stream Mach number.

Gust plates were sized to provide nominal gust Mach numbers of 0.05 and 0.1 at the clean (no plate) tunnel Mach numbers of 3.1 and 2.4. These values for the gust were chosen for convenience of testing and evaluation of the gust plate concept. They were not intended to duplicate any specific gust conditions that are present at any specific flight Mach number or altitude. Sizing of the plates were based on the calibrated nozzle area change for test section Mach number variation. The Mach 2.4 gust plates were also tested at Mach 2.0.

U.S. Customary Units were used in the design of the test models and for recording and computing of data. These units were converted to the International System of Units for presentation in this report.

APPARATUS AND PROCEDURE

General Description of Wind Tunnel

A schematic diagram of the Lewis 10- by 10-Foot Supersonic Wind Tunnel is presented in figure 1. A diagram of the flexible-wall nozzle and test section is shown in figure 2. Ceiling and floor surfaces are parallel from the entrance of the nozzle to a station downstream of the test section. The tunnel height (3.048 m) was used to nondimensionalize most of the dimensions that are presented in this report.

Coordinates for the nozzle and test section walls are presented in table I. In this table nozzle wall Mach number M_w refers to the geometric positioning of the flexible nozzle walls. (Symbols are defined in appendix A.) This wall Mach number is only a nominal indication of the free stream condition that was obtained in the test section. During design and initial calibration of the wind tunnel, the nozzle wall contour was adjusted to compensate for boundary layer growth; therefore, the area ratio of nozzle throat area to test section area does not correlate with the ideal nonviscous area ratio for an indicated wall Mach number. The actual (no gust plate installed) calibrated Mach number $\left(\text{referred to in this report as } M_{cal}\right)$ can vary a small amount from the nominal nozzle wall value due to different amounts of boundary layer buildup on the walls for different Reynolds number test conditions. This calibrated Mach number was based on an average of the free stream Mach numbers in a 1.219-meter square in the center of the test section. Since the addition of the gust plate modifies the original flexible nozzle airflow characteristics, neither the nominal wall Mach number nor the calibrated Mach number were obtained in the test section during this investigation. However, since the wall Mach number does indicate a particular nozzle wall geometry, this parameter will be used in the text and figures of this report as an indication of both the nozzle wall geometry and the nominal (no gust plate installed) test conditions.

Gust Plate Configurations

Gust plate details are shown in figure 3. The conceptual installation of a gust generator in the nozzle throat of a wind tunnel is shown in figure 3(a). Plate rotation about its centerline would be provided by some type of drive system. Although only a floor mounted system is shown, a duplicate of this system that would be installed on the nozzle ceiling would probably be required to eliminate asymmetric airflow conditions in the test section. As indicated in figure 3(b) the gust plates for this study were installed at the geometric throat of the tunnel nozzle and were installed on the floor of the tunnel. The sizes of the gust plates and their vertical positions above the tunnel floor are shown in figure 3(c). Multiple-symbol designations for the gust plate configurations are used to indicate the plate size, position, and design Mach number. The first symbol represents plate height; L denotes large and S denotes small. Since the plates for a given Mach number were the same width, the first symbol also indicates the intended nominal Mach number decrement of 0.05 for S and 0.10 for L. The second symbol indicates that the plate was mounted on the floor (denoted by Z) or above the floor (denoted by A). Number designations for the third symbol represented the nozzle wall Mach number for which the gust plates were designed. Basically the gust plates were sized for Mach number decrements of 0.05 and 0.10 to Mach numbers of about 2.4 and 3.1. The Mach 2.4 gust plates were also tested with the nozzle set at the Mach 2.0 position. The values of gust Mach number were chosen for convenience of testing and evaluation of the gust plate

concept. They were not intended to duplicate any specific gust conditions that are present at any particular flight Mach number or altitude. The sizing of the plates was based on the calibrated nozzle area change for test section Mach number variation. All of the gust plates were fixed in the vertical position except for configuration LZ2.4. This plate was hinged at the bottom. Steady-state data were obtained with this plate locked in the vertical position. To obtain the single transient data point, the plate was released and allowed to rotate about the bottom hinge until it hit the nozzle floor. Mach 3.1 and 2.4 gust plate widths were selected to allow a gap of about 3.8 centimeters to provide clearance between the end of the plate and the nozzle wall. Distance between the nozzle walls increases when they are moved from Mach 2.4 to 2.0 positions; therefore, a gap of about 30.1 centimeters between the end of the plate and the wall was obtained when the Mach 2.4 gust plates were tested at a nozzle wall Mach number setting of 2.0. The large plates (L) were tested on and above the tunnel floor. This height that the plate was positioned above the floor (d/H = 0.0833, fig. 3(c)) was chosen for convenience and was not based on an extensive analysis of the local airflow conditions.

Instrumentation

Nozzle and test section ceiling static pressure instrumentation locations are presented in table II. The location of the wind tunnel bellmouth total pressure instrumentation is shown in figure 2.

Although the test section is 12.18 meters long, only the local airflow conditions in the region of the upstream schlieren window (fig. 2) were measured. Data at four survey rake positions (x/H of 5.42, 5.62, 5.87, and 6.22) were obtained. Arrangement of the calibration wedges on the rake is shown in figure 4(a). Wedges 1 to 9 were instrumented with steady-state pressure tubes and dynamic pressure transducers were installed in wedges 10 and 11. Details of the calibration wedges are shown in figures 4(b) and 4(c).

Data Reduction

Because the flow angles and distortions were somewhat larger for this test than usual, a more accurate calculation of the Mach number and flow angle at each calibration wedge was required. Normally, the average value of P_1 and P_3 (see fig. 4(b)) were used to determine Mach number, and the difference between p_2 on the upper surface and p_2 on the lower surface was used for flow angle. For this test a free stream Mach number and deflection angle were determined for the upper surface, using P_1, p_2, and P_3 on the upper surface. A similar calculation was made for the lower surface. From the known effective wedge half-angle of 20.5° and the flow deflection angle a free stream flow angle can be determined for each surface. Because of small inaccuracies in the pressure measurements the two (top and bottom) Mach numbers and the two flow angles

4

were not identical, so that an average value of each quantity was used. A more detailed explanation of the analysis is given in appendix B.

<div align="center">RESULTS AND DISCUSSION</div>

This part of the report is presented in four sections. The first, second, and third sections are a presentation of data that were obtained for the three test nozzle wall Mach number settings of 3.1, 2.4, and 2.0, respectively. In the fourth section a discussion of the typical oblique shocks that are obtained for the various test Mach numbers is presented.

<div align="center">Wall Mach Number of 3.1</div>

Local test section conditions that were obtained for gust plate LA3.1 are presented in figure 5. For these data the gust plate was fixed in the vertical or maximum blockage position. Local Mach number, airflow angle, and total pressure recovery profiles in the vertical direction for four survey rake stations are presented. Figure 5 is representative of the plots that are used for the presentation of the local test section conditions for all of the gust plate configurations. Variations of local airflow conditions in the lateral direction are not presented on separate plots; however, an indication of the lateral variation of the parameters can be determined by comparing the multiple symbols that are shown for the top and bottom of the rake for each rake station. For example, the variation in Mach number between wedges 1, 6, and 2 at a rake station x/H of 5.62 is represented by the three diamond-shaped symbols at a vertical height ratio h/H of 0.7 in figure 5(a).

Data that are presented in figure 5(a) show that the airflow accelerates through the region of survey. On the tunnel centerline ($h/H = 0.5$), the local Mach number increases from 3.067 at a rake station of 5.42 to a Mach number of 3.222 at rake station 6.22. The acceleration of the test section airflow in the axial direction that are obtained for a clean (no gust plate) tunnel is insignificant when compared to the large values that are shown in figure 5(a). Local Mach numbers for plate configuration LA3.1 in a horizontal position were not obtained; however, it is reasonable to assume that a local Mach number would be close to the calibrated (clean tunnel) Mach number if the plate was rotated to the horizontal position. The calibrated (clean tunnel) Mach number is indicated in figure 5(a). Therefore, if a gust Mach number of about 0.1 is required a test model must be positioned near station 6.22. At this station a Mach number of 3.2 would be obtained with plate LA3.1 in the vertical position and a Mach number of about 3.1 would be obtained by rotating the plate to a horizontal position. These data indicate that a gust plate system can conceptually be used to provide Mach number changes in a given portion of the test section.

With gust plate LA3.1 in the vertical position, figure 5(b) shows a variation of local airflow angle from about negative 2° at the top of the rake ($h/H = 0.7$) to negative 4° at the bottom of the rake ($h/H = 0.3$). During normal tunnel operation (no gust plates), the

local airflow angle in the test section is nominally 0°. The local airflow angle should approach this value as the gust plate is rotated to the horizontal position; therefore, rotation of the flat-plate gust generator will result in variation in airflow angle and Mach number. Since the total pressure recovery without a generator is nominally 0.98 and figure 5(c) shows reduced levels of total pressure recovery with the gust plate in the vertical position, a variation in test section total pressure will also occur with gust plate rotation.

Although a gust that is encountered by an aircraft may result in combined variations of Mach number, angle of attack, and pressure levels, the gust generator for the wind tunnel was intended to provide only a variation in free stream Mach number. Multiple variations that are caused by the gust generator do not allow the effects of single components of a gust to be investigated. Variation of the local airflow angle could most likely be eliminated if a gust plate was also installed on the ceiling of the tunnel throat. The downflow that is obtained with the floor gust plate would be cancelled by an upflow from the ceiling gust plate. These gust plates would be reduced in size to maintain an equivalent blockage to the original (one plate) configuration. The variation in local total pressure level as the plate rotates from vertical to horizontal positions cannot be eliminated. Total pressure level changes are the result of changes in oblique shock wave patterns that are obtained with the gust plate. The oblique shock wave patterns are discussed in the Wall Mach Number of 2.4, Wall Mach Number of 2.0, and Typical Oblique Shocks sections of this report.

The effect of Reynolds number on local test section conditions at rake station x/H of 6.22 for configuration LA3.1 and a wall Mach number of 3.1 is shown in figure 6. Figure 6(a) shows a reduction in local Mach number as the Reynolds number was reduced. At a wall Mach number of 3.1 with no gust plate, the free stream Mach number decreases about 0.025 when the Reynolds number is decreased from 8.37 to 4.07 million per meter. Therefore, the Mach number reduction (fig. 6(a)) was mainly the result of the normal trend of reduced Mach number with a decrease in Reynolds number.

Local test section conditions that are presented in figure 7 for plate SZ3.1 and a wall Mach number of 3.1 show similar trends to those that were obtained for plate LA3.1 of figure 5.

Nozzle and test section ceiling static pressure distributions for plates LA3.1 and SZ3.1 are presented in figure 8.

Wall Mach Number of 2.4

Local airflow conditions that were obtained in the wind tunnel test section for the Mach 2.4 gust plates are presented in figures 9 to 18. Data for three gust plates (LZ2.4, LA2.4, and SZ2.4) are shown.

Local test section conditions that were obtained for plate LZ2.4 in the maximum blockage position are shown in figure 9. The data in figure 9 was obtained with the survey

6

rake rotated 90°. This rotation allowed airflow angles in the lateral plane to be determined. Airflow angles were found to be nominally zero and are not presented. Airflow angles in the vertical plane, Mach number, and total pressure recovery (before and after rotation of plate LZ2.4) are presented in figure 17 and are discussed near the end of this section of the report. Figure 9(a) shows that the airflow at the top of the survey rake (h/H = 0.7) accelerates through the region of survey. The top of the survey rake was always in a region of higher Mach number upstream of an oblique shockwave. This shockwave is shown in figure 10. The dark vertical line in the schlieren photograph was the result of a wire in front of the schlieren window. Sharp discontinuities in the local Mach number as shown in figure 9(a) was the result of the oblique shock. Data for all of the survey rake wedges at each rake station are not presented. If the oblique shock intersected the wedge instrumentation, the data for that wedge are not shown. Data that are presented indicate that local Mach numbers greater than the nominal Mach number of 2.5 which was used for sizing the large plate were obtained. Mach numbers larger than the 2.5 level indicate that the effective blockage area of the plate was larger than the physical area.

The effect of a variation in Reynolds number on local test section Mach number at rake station x/H of 5.42 for plate LZ2.4 and nozzle wall Mach number setting of 2.4 is presented in figure 11. Schlieren photographs and data (not included) indicate that the oblique shock moves upstream as the Reynolds number was reduced. This trend is indicated in figure 11 by an upward shift of the discontinuity in the local Mach number profile. The small decrease in Mach number that was obtained when the Reynolds number was reduced was the result of normal tunnel characteristics and was not the result of the gust plate installation.

Data that were obtained for gust plate configuration LA2.4 in the vertical position at a wall Mach number of 2.4 are presented in figure 12. These data are similar to the data that were obtained for gust plate LZ2.4 (fig. 9). Comparison of figures 9(a) and 12(a) indicates that the local Mach number upstream of the oblique shock was higher for gust plate LA2.4 than for gust plate LZ2.4. For example, at a vertical height ratio h/H of 0.7, the triangular symbols in figure 12(a) (plate LA2.4) indicate a local Mach number of about 2.61 while these symbols show a local Mach number of about 2.55 for plate LZ2.4 in figure 9(a). This increased Mach number for configuration LA2.4 could be the result of an increase in effective blockage of the nozzle throat when the gust plate was located 0.254 meters above the floor (plate LZ2.4 to plate LA2.4). Comparison of schlieren photographs of figure 10 (plate LZ2.4) and 13 (plate LA2.4) shows that locating the large gust plate above the tunnel floor also results in an upstream movement of the oblique shock. Examination of the Mach number profiles in figures 9(a) and 12(a) also shows this upstream shock movement. The change in local airflow angle through the oblique

shock can be seen in figure 12(b) for plate LA2.4 with downflow or negative angles upstream and upflow downstream of the shock.

Data presented in figure 14 for the small plate configuration SZ2.4 shows that only a small part of the region of survey was in the higher Mach number region upstream of the oblique shock. Decreasing the height of plate LZ2.4 by one-half to obtain plate SZ2.4 (fig. 3) resulted in an upstream movement of the oblique shock to a position ahead of the schlieren window. Since the shock was not in the window region, schlieren for configuration SZ2.4 are not presented. Comparison of the local Mach numbers upstream of the oblique shock in figures 9(a) and 14(a) indicates that the reduced plate height did not substantially reduce the local test section Mach number.

Location of the oblique shocks that were obtained for plates LZ2.4, LA2.4, and SZ2.4 when tested at a wall Mach number of 2.4 are shown in a sketch of part of the nozzle and test section in figure 15. This figure shows that the oblique shock moved upstream if the plate was positioned above the nozzle floor (LZ2.4 to LA2.4) or if the plate height was reduced (LZ2.4 to SZ2.4). Figures 9, 12, and 14 have shown that the Mach number upstream of the oblique shock was nominally 2.57 while downstream of the shock the Mach number was about 2.4. Therefore, if a test model is to be mounted on the tunnel centerline (h/H = 0.5) and be located in the region of higher Mach number (M_l = 2.57) prior to an airflow gust, figure 15 indicates that gust plate LZ2.4 must be used. The use of plates LA2.4 or SZ2.4 would require that the model be mounted upstream of the test section. This upstream positioning of a model would probably be difficult to provide with a mounting system that has basically been designed for mounting of test models in the test section.

Nozzle and test section ceiling centerline static pressures for plates LZ2.4, LA2.4, and SZ2.4 are presented in figure 16. The pressure rise at an x/H of about 2.0 was the result of an oblique shock intersecting the ceiling. Evidently this oblique shock was generated from the gust plate flow field. The effect of this shock as it reflected downstream to the test section has been shown.

Figure 15 has indicated that plate LZ2.4 was the most desirable plate configuration of those that were tested for the wall Mach 2.4 condition. Therefore, to investigate the dynamic characteristics of the wind tunnel and to obtain steady-state data for maximum and minimum blockage, this plate was mounted with hinges at the bottom and released from the upright position. This transient corresponds to rotating a paddle wheel through an angle of 90°.

Local test conditions before and after rotation of gust plate LZ2.4 are shown in figure 17. The local Mach number (fig. 17(a)) decreased by 0.15 (M_l = 2.57 to 2.42) at the centerline of the test section (h/H = 0.5). The discontinuity in Mach number between the two lower rake stations with the gust plate vertical indicates the presence of an

8

oblique shock wave. With the plate horizontal no such discontinuity is present, indicating that the oblique shock wave has moved out of the survey rake field or is no longer present in the test section. The presence of this oblique shock wave did affect the dynamic pressure measurements on wedge 11.

Figure 17(b) shows that the local airflow angle was reduced by 2.9^O ($\alpha_l = -3.9^O$ to -1.0^O) when gust plate LZ2.4 was rotated from the vertical to the horizontal position. The airflow angularity with the plate horizontal was less than 1.5^O indicating that the effect of the oblique shock is decreased as would be expected since the gust plate is essentially removed from the tunnel. The local pressure recovery (fig. 17(c)) increased by 0.036 ($P_l/P_{BM} = 0.955$ to 0.991) when the plate was dropped from the vertical to the horizontal position. The static pressure distribution on the nozzle and test section ceiling centerline is presented in figure 17(d). Again a discontinuity is present in this profile with the plate in the vertical position showing the reflection point of the oblique shockwave.

The transient conditions which occurred during rotation of plate LZ2.4 were obtained using pressure transducers D_1 to D_4 on wedges 10 and 11. These signals and a plate angular position signal were recorded on magnetic tape and are presented in figure 18. Each pressure signal was recorded twice: a low gain recording to observe general changes in the signals, and a high gain recording to provide details of the transient. As seen in figure 18, the high gain trace for D_1 saturated a recording amplifier near the completion of the transient. Also the high noise spikes on the plate angular position trace result from failure of the position indicator when the plate hit the nozzle floor.

The plate rotated from the vertical to the horizontal position in about 15 milliseconds. The pressures on wedge 10 (D_1 and D_2) responded to the disturbance about 50 milliseconds after the release point. The responses of these pressures are of interest because they are located in the region of higher local Mach number upstream of the oblique shock wave (see fig. 17(a)). The responses of wedge 11 pressures (D_3 and D_4) are difficult to interpret in terms of change in Mach number since the wedge is near and apparently crossed by an oblique shock wave.

The static pressure on wedge 10 (D_1) required roughly 20 milliseconds to reach 63 percent of its final value. If the transient is assumed to be a first-order step response, this time period corresponds to the time constant. A first-order lag with a time constant of 20 milliseconds has a corner frequency (-3 dB) of 8 hertz. However, the plate position is not an ideal step input since it takes 15 milliseconds to drop. This makes interpretation of the pressure response for frequencies beyond the highest input frequency impossible. Therefore, the dynamic transients recorded in figure 18 indicate that the tunnel will respond to at least 8 hertz when a rotating paddle wheel is used.

Local airflow conditions that were obtained with the nozzle walls set at the Mach 2.0 position, for the gust plates which were sized for a nozzle wall setting of Mach 2.4 are presented in figures 19 to 26.

Local test section conditions that were obtained for plate LZ2.4 in the vertical position and a wall Mach number of 2.0 are shown in figure 19. The survey rake was rotated 90°; therefore, airflow angles are not presented. Figure 19(a) shows that the airflow accelerates through the region of survey at the bottom (h/H = 0.3) of the survey rake. The local Mach number increases from about 2.07 at an x/H of 5.42 to about 2.13 at a survey rake station x/H of 6.22. This trend was also obtained for the other two test Mach numbers $\left(M_w = 3.1 \text{ and } 2.4 \right)$. Discontinuities in the Mach number profiles for rake stations x/H of 5.87 and 6.22 (fig. 19(a)) and a schlieren photograph (fig. 20) indicate that an oblique shock was present. For the wall Mach 2.4 test condition of plate LZ2.4 it was shown that the local Mach number approaches the nominal Mach number when the plate was rotated from the vertical to horizontal position (fig. 17). This trend should be the same for the Mach 2.0 wall test conditions. Therefore, figure 19(a) indicates that a gust Mach number of about 0.075 $\left(M_l = 2.075 \text{ to } 2.0 \right)$ could be provided at rake station 5.42 by rotating gust plate LZ2.4. Plate LZ2.4 was sized to provide a change in Mach number of about 0.1 at a wall Mach number of 2.4. Since the throat area change for a 0.1 Mach number variation at a wall Mach number of 2.0 was much larger than for a wall Mach number of 2.4, it was expected that plate LZ2.4 would provide a gust Mach number less than 0.1 when tested at wall Mach 2.0.

Figure 19(a) shows that the top part of the rake, when positioned at the two downstream rake stations, was influenced by an oblique shock. Comparison of figure 10 $\left(M_w = 2.4 \right)$ and figure 20 $\left(M_w = 2.0 \right)$ for plate LZ2.4 shows the effect of changing the wall Mach number on the oblique shock. For a wall Mach number of 2.4, the oblique shock was reflected from the tunnel floor up through the region of survey while it was reflected down through the region of survey at a wall Mach number of 2.0. This change in direction was the result of the reflection point at an x/H of 7.05 (fig. 15) for a wall Mach number of 2.4 moving upstream to an x/H of 5.2 when the wall Mach number was reduced to 2.0. The resulting oblique shock from this reflection point on the ceiling (x/H = 5.2) extends downward through the region of survey.

The effect of a variation in the Reynolds number on local test section Mach number at rake station x/H of 5.42 for plate LZ2.4 and a Mach number of 2.0 is presented in figure 21. The small decrease in local Mach number when the Reynolds number was reduced was the result of the normal tunnel characteristics and was not the result of gust plate installation.

Data that were obtained for plate LA2.4 when tested at a wall Mach number of 2.0 are presented in figures 22 and 23. These data are similar to the data for plate LZ2.4 when tested at the same conditions. Comparison of the circular symbols in figures 19(a) and 22(a) indicates that a larger part of the survey rake was in the lower Mach number region (downstream of the oblique shock) for plate LA2.4 than for LZ2.4. This indicates that the oblique shock moved upstream when the plate was positioned above the nozzle floor.

Figure 22(b) shows that positive airflow angles greater than 2° were obtained in the region upstream of the oblique shock. As discussed previously and shown in figure 17(b), the airflow angle should approach 0° when the plate is rotated to the minimum blockage position. The positive airflow angles for wall Mach 2.0 test conditions and negative airflow angles for wall Mach 2.4 test conditions was the result of airflow turning through the reflecting-oblique shock system when the plates were in the vertical position. Schlieren photographs for plate LA2.4 are shown in figure 23.

Gust plate SZ2.4 data are presented in figure 24. Comparison of the local Mach numbers at rake station 5.42 upstream of the oblique shock in figure 24(a) and 19(a) indicates that a 50 percent reduction in plate height from LZ2.4 to SZ2.4 did not substantially reduce the local Mach number. Comparison of the Mach number profiles at rake station 6.22 in these two figures also shows that the oblique shock moved upstream when the smaller plate (SZ2.4) was installed.

The locations of the oblique shocks that were obtained with the Mach 2.4 gust plates when tested at a wall Mach number of 2.0 are shown in figure 25. This figure shows that the oblique shock furthest downstream was obtained with plate LZ2.4. As pointed out in the discussion of the similar figure for wall Mach 2.4 test conditions (fig. 15), this downstream shock position is desirable when mounting of a test model must be considered. For both test conditions $\left(M_w = 2.4 \text{ and } 2.0\right)$, plate LZ2.4 provided the most downstream oblique shock location. Even though the most downstream oblique shock was obtained with plate LZ2.4, data for this configuration indicate that, for nominal local Mach 2.5 and 2.1, free stream conditions in the test section prior to an airflow gust the test model must be mounted near the beginning of the test section to avoid the oblique shock waves that exist for these two test conditions. The oblique shock reflection points on the ceiling between an x/H of about 4.8 and 5.2 in figure 25 can be seen as a pressure rise at these stations in figure 26. Figure 26 presents the nozzle and test section ceiling static pressure distributions for the three Mach 2.4 gust plates when tested at a Mach number of 2.0. This figure indicates two shock reflection locations on the nozzle ceiling for the Mach 2.0 test conditions. The first reflection point was at an x/H of about 1.5. Since additional instrumentation was not located in this region, the exact reflection point cannot be determined for each of the configurations. Reflection

points are shown for each plate at an x/H of about 5.0. These locations were determined from an analysis of the pressure distributions and plots like figure 25.

Typical Oblique Shocks

A sketch of the typical oblique shock systems that are obtained for gust plates mounted on the nozzle floor for wall Mach numbers of 2.0, 2.4, and 3.1 is presented in figure 27. Just downstream of the gust plate it was assumed that a separated flow region (caused by the plate) attached to the tunnel floor. Reflection points where the oblique compression shocks intersect the tunnel ceiling were determined from pressure distribution plots that are presented in figures 8, 16, and 26 $\left(M_w = 3.1, \quad 2.4, \quad \text{and} \quad 2.0, \right.$ respectively$\left. \right)$. Although figure 27 shows typical shock systems, data for gust plates LA3.1 $\left(M_w = 3.1 \right)$ and LZ2.4 $\left(M_w = 2.4 \quad \text{and} \quad 2.0 \right)$ were selected for presentation. The first reflection point on the floor for wall Mach 2.0 conditions was estimated; however, the remaining part of the shock system was based on test data as shown in figures 25 and 26. As shown in figure 27 by the solid line, the first reflection point on the tunnel floor and the remaining shock system for wall Mach 2.4 are based on measured data. Oblique shock locations that were obtained for this test condition are presented in figure 15. Oblique shocks were not observed in the region of survey for a wall Mach number of 3.1; therefore, the shock system downstream of the first ceiling reflection point for this Mach number was estimated.

SUMMARY OF RESULTS

An investigation was conducted to determine the effectiveness of a flat plate gust generator that was located in the nozzle throat of the Lewis 10- by 10-Foot Supersonic Wind Tunnel. Gust plates were tested at three Mach numbers that are representative of the Mach number range of the tunnel. The effect of plate height, vertical location of the plate above the nozzle floor, and Reynolds number was investigated. The following results were obtained:

1. Data show that a change in free stream Mach number, a change in airflow angle and total pressure recovery were obtained in the test section of the wind tunnel by rotating a flat plate in the throat of the supersonic nozzle. Steady-state conditions before and after a gust that was created by allowing a gust plate (LZ2.4) to rotate from a vertical to a horizontal position indicate that the test section centerline Mach number decreased 0.15 $\left(M_l = 2.57 \quad \text{to} \quad 2.42 \right)$, the local airflow angle changed from -3.9^o to -1.0^o, and the total pressure recovery increased from 0.955 to 0.991.

2. With the gust plate mounted in a vertical position, the test section airflow in general tended to accelerate through the region of survey for the three nominal test Mach

numbers. This airflow acceleration occurred upstream of an oblique shock wave that was in the region of survey for test wall Mach numbers of 2.0 and 2.4.

3. At the nominal Mach 2.5 and 2.1 free stream conditions in the test section prior to an airflow gust, the test model must be mounted near the beginning of the test section to avoid an oblique shock wave that exists for these two test conditions.

4. During steady-state conditions prior to a gust disturbance, the oblique shock that was in the test section for nominal local Mach numbers of 2.5 and 2.1 moved upstream when a 0.305-meter-high gust plate was mounted 0.254 meters above the floor or when the plate height was reduced by 50 percent.

5. During an airflow disturbance that was created by rotating a gust plate in the nozzle throat, the test section pressures lagged the initiation of the disturbance in the throat by 50 milliseconds. The gust plate rotated from the vertical to the horizontal position in 15 milliseconds while about 35 milliseconds were required for the pressures in the airflow region upstream of the oblique shock to change from the initial to the final value. From the beginning of static pressure level change in the test section, 63 percent of the pressure change occurred in the first 20 milliseconds. This corresponds to a corner frequency of 8 hertz for an ideal step input. Since the input transient was 15 milliseconds long, the actual response may be greater than 8 hertz.

6. The effective blockage area of the gust plate was larger than the physical blockage area.

Lewis Research Center,
National Aeronautics and Space Administration,
Cleveland, Ohio, July 17, 1974,
501-24.

APPENDIX A

SYMBOLS

d	height of gust plate bottom edge above nozzle floor
g	gust plate height
H	height of test section, 3.048 m
h	vertical distance from tunnel floor
l	gust plate width
M	Mach number
P	total pressure
p	static pressure
R_N	Reynolds number per meter (calculated by using tunnel supersonic nozzle wall position nominal Mach number)
t	gust plate thickness
x	axial distance from nozzle geometric throat, positive downstream
y	lateral distance from tunnel centerline to tunnel sidewall
α	airflow angle (positive angle indicates an upflow), deg
γ	ratio of specific heats
δ	turning angle
θ	wedge lip shock angle

Subscripts:

BM	nozzle bellmouth
cal	calibrated
l	local
w	nozzle wall position
0	free stream
1	local free stream pitot pressure
2	calibration wedge surface
3	calibration wedge surface pitot pressure

APPENDIX B

DATA REDUCTION PROCEDURE FOR CALIBRATION WEDGES

Because the flow angles and distortions were somewhat larger for this test than experienced in previous tests (ref. 5), a more accurate calculation of the Mach number and flow angle at each calibration wedge was required. Six pressure measurements are made at each wedge (fig. 4(b)): two (top and bottom) static pressures on the surface of the wedge p_2, two (top and bottom) total pressures behind the leading edge shock P_3, and two total pressures in the free stream P_1. The two free stream pressures are averaged so that only five separate pressure values are determined for each wedge. From these five values two separate calculations for the free stream Mach number and the free stream flow angle are made.

From the values of p_2 and P_3 on the upper surface of the wedge, the Mach number M_2 on the upper surface behind the lip shock can be determined

$$\frac{P_3}{p_2} = \left[\frac{(\gamma + 1)M_2^2}{2}\right]^{\gamma/(\gamma-1)}\left[\frac{\gamma + 1}{2\gamma M_2^2 - (\gamma - 1)}\right]^{1/(\gamma-1)} \tag{B1}$$

where γ is ratio of specific heats. A value for γ of 1.4 is used in all calculations. Equation (B1) is solved iteratively for M_2 when P_3/p_2 is known.

The local free stream Mach number and flow angle are found using an iterative scheme. An initial guess is made for the local free stream Mach number M_l. If M_l and P_1 are known, the free stream total pressure P_l can be found

$$\frac{P_1}{P_l} = \left[\frac{(\gamma + 1)M_l^2}{(\gamma - 1)M_l^2 + 2}\right]^{\gamma/(\gamma-1)}\left[\frac{\gamma + 1}{2\gamma M_l^2 - (\gamma - 1)}\right]^{1/(\gamma - 1)} \tag{B2}$$

From P_l and p_2 the wedge lip shock angle θ can be determined as

$$\sin^2\theta = \frac{(\gamma - 1) + \left(\dfrac{p_2}{P_l}\right)(\gamma + 1)\left[\dfrac{(\gamma - 1)M_l^2 + 2}{2}\right]^{\gamma/(\gamma - 1)}}{2\gamma M_l^2} \tag{B3}$$

The turning angle δ of the flow on the upper surface can now be determined

$$\tan \delta = \frac{M_l^2 \sin 2\theta - 2 \cot \theta}{2 + M_l^2(\gamma + \cos 2\theta)} \tag{B4}$$

Knowing δ, θ, and M_2, a new estimate for M_l can be found

$$M_l^2 = \frac{2 + (\gamma - 1)M_2^2 \sin^2(\theta - \delta)}{\sin^2\theta \left[2\gamma M_2^2 \sin^2(\theta - \delta) - (\gamma - 1)\right]} \tag{B5}$$

The new estimate for M_l is used to find new values for P_l, θ, and δ. This iterative procedure is continued until two successive values of M_l differ by a sufficiently small amount. Since the wedge half-angle is known, a simple subtraction of this half-angle from δ gives the local flow angle. Thus, the local free stream Mach number and flow angle can be determined from the two pressure measurements on the upper surface of the wedge and the free stream pressure measurements P_1.

A similar calculation is made for the two pressure measurements on the lower surface of the wedge, so that two independent calculations for local free stream Mach number and flow angle are made at each wedge. Because of small inaccuracies in the pressure measurements the two calculations do not give identical values, so the average of the two calculations was used.

16

REFERENCES

1. Wasserbauer, Joseph F.: Dynamic Response of a Mach 2.5 Axisymmetric Inlet with Engine or Cold Pipe and Utilizing 60 Percent Supersonic Internal Area Contraction. NASA TN D-5338, 1969.

2. Choby, David A.: Tolerance of Mach 2.50 Axisymmetric Mixed-Compression Inlets to Upstream Flow Variations. NASA TM X-2433, 1972.

3. Mitchell, Glenn A.; and Sanders, Bobby W.: Pressure-Activated Stability-Bypass-Control Valves to Increase the Stable Airflow Range of a Mach 2.5 Inlet with 40-Percent Internal Contraction. NASA TM X-2972, 1974.

4. Investigation of Supersonic Transport Engine Inlet Configurations. Rep. No. 19014, Lockheed Aircraft Corp., Sept. 1965.

5. Cubbison, Robert W.; and Meleason, Edward T.: Water Condensation Effects of Heated Vitiated Air on Flow in a Large Supersonic Wind Tunnel. NASA TM X-1636, 1968.

TABLE I.- NOZZLE AND TEST SECTION COORDINATES

Axial station, x/H	Nozzle wall Mach number, M_w		
	2.0	2.4	3.1
	Lateral distance from tunnel centerline, y/H		
-1.9250	0.3755	0.3574	0.3389
-1.6500	.3557	.3225	.2859
-1.3583	.3361	.2881	.2334
-1.0666	.3188	.2577	.1870
-.7750	.3045	.2327	.1490
-.4917	.2941	.2145	.1214
-.2458	.2883	.2045	.1061
0	.2863	.2009	.1005
.2458	.2883	.2044	.1053
.5000	.2941	.2144	.1199
.7833	.3048	.2325	.1460
1.0750	.3194	.2572	.1812
1.3500	.3360	.2848	.2199
1.5708	.3508	.3092	.2532
1.7833	.3667	.3347	.2866
1.9958	.3832	.3604	.3197
2.2080	.4002	.3864	.3512
2.4375	.4188	.4124	.3817
2.6833	.4385	.4358	.4101
2.9583	.4576	.4562	.4363
3.2417	.4756	.4715	.4573
3.5250	.4832	.4821	.4727
3.8083	.4895	.4888	.4832
4.0917	.4925	.4923	.4898
4.3833	.4943	.4942	.4945
4.6750	.4957	.4956	.4960
4.9667	.4980	.4979	.4982
5.2583	.5000	.5000	.5000
Test section	0°22" sidewall divergence		
9.2583	0.5258	0.5258	0.5258

TABLE II.- NOZZLE AND TEST SECTION CEILING CENTERLINE

STATIC PRESSURE INSTRUMENTATION LOCATIONS x/H

-0.0120	3.0125
.0104	3.6958
.0625	4.3793
.2083	4.9083
.3625	5.1083
.6625	5.2083
1.0625	5.3083
1.7125	5.5083
2.3542	
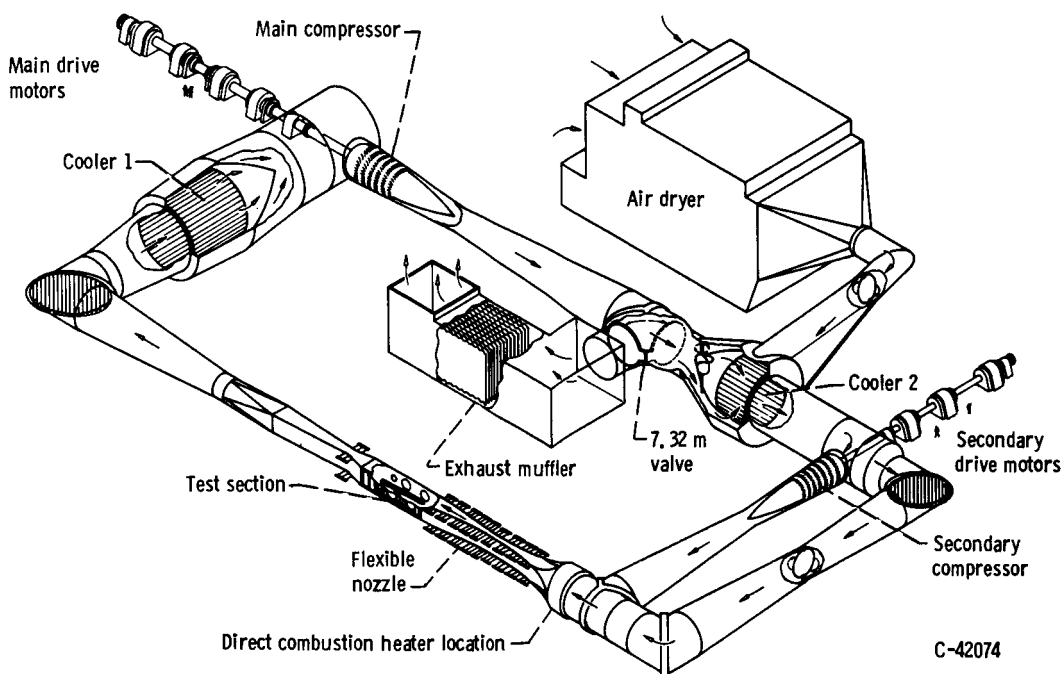
Figure 1. - Schematic diagram of Lewis 10- by 10-Foot Supersonic Wind Tunnel.
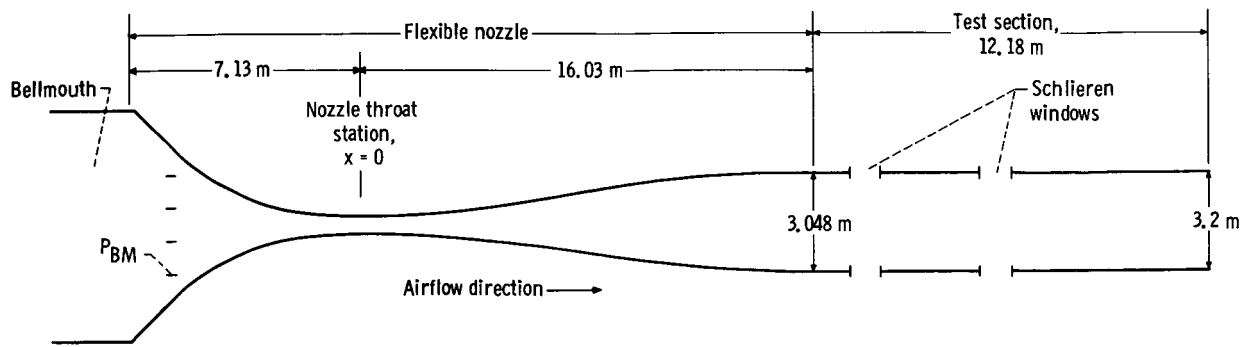
Figure 2. - Schematic diagram of wind tunnel bellmouth, nozzle, and test section.
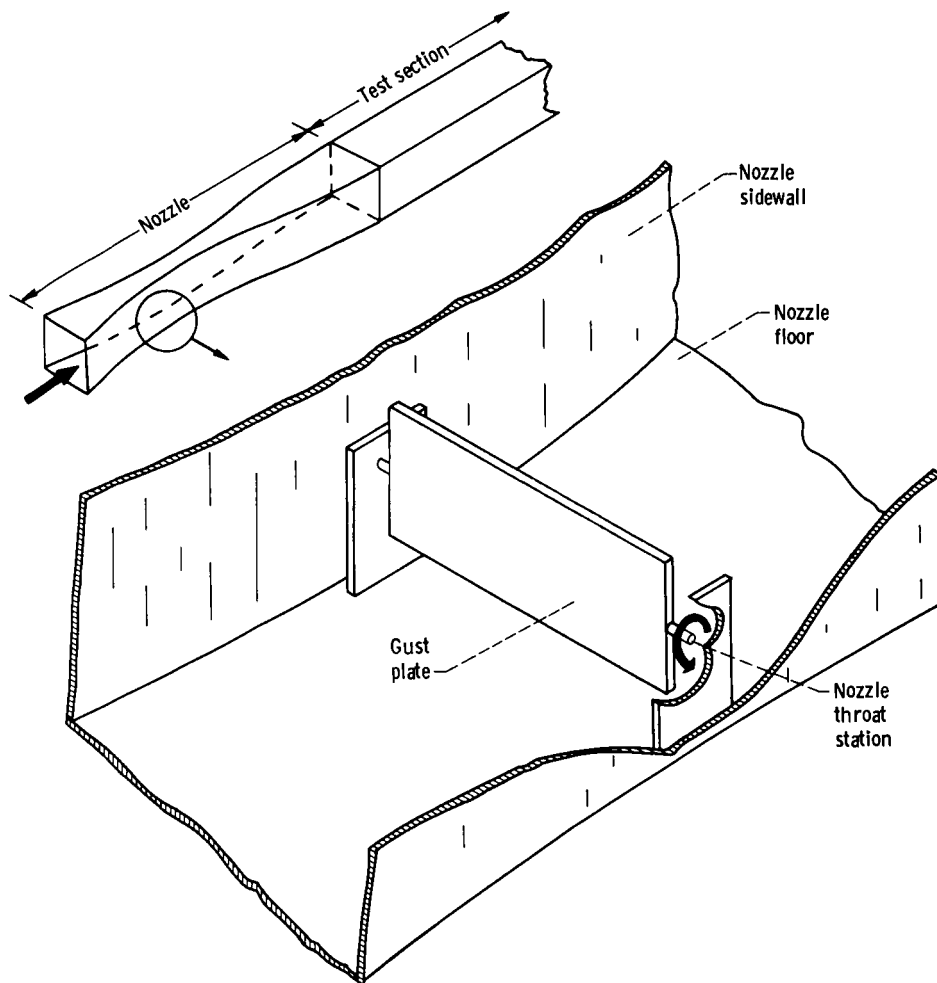
(a) Sketch of potential gust generator system in nozzle throat of a wind tunnel.

Figure 3. - Gust plate details.
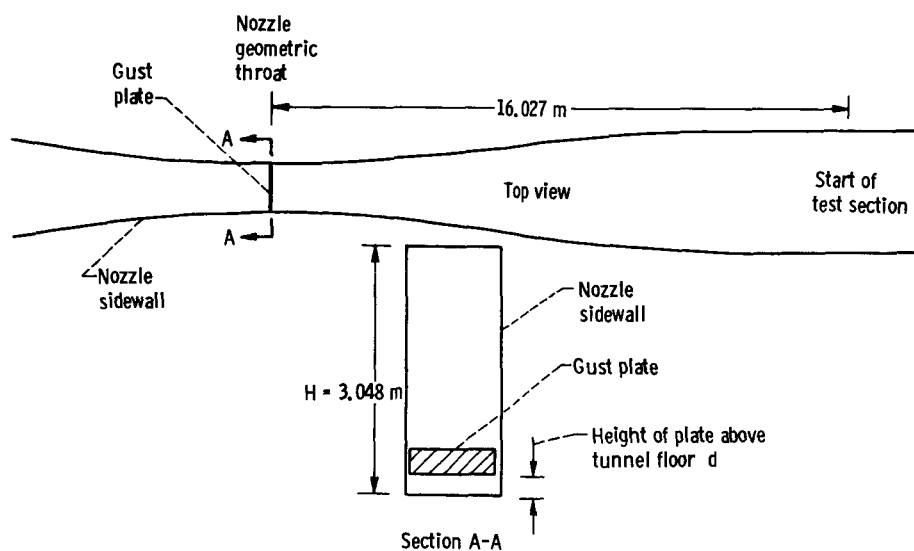
(b) Location of gust plate in tunnel nozzle.
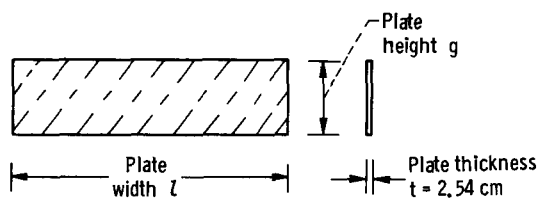
Gust plate configuration	Plate width ratio, l/H	Plate height ratio, g/H	Plate vertical position ratio, d/H
LA3.1	0.175	0.10	0.0833
SZ3.1	.175	.05	0
LZ2.4	.375	.10	0
LA2.4	.375	.10	.0833
SZ2.4	.375	.05	0

(c) Gust plate configurations.

Figure 3. - Concluded.
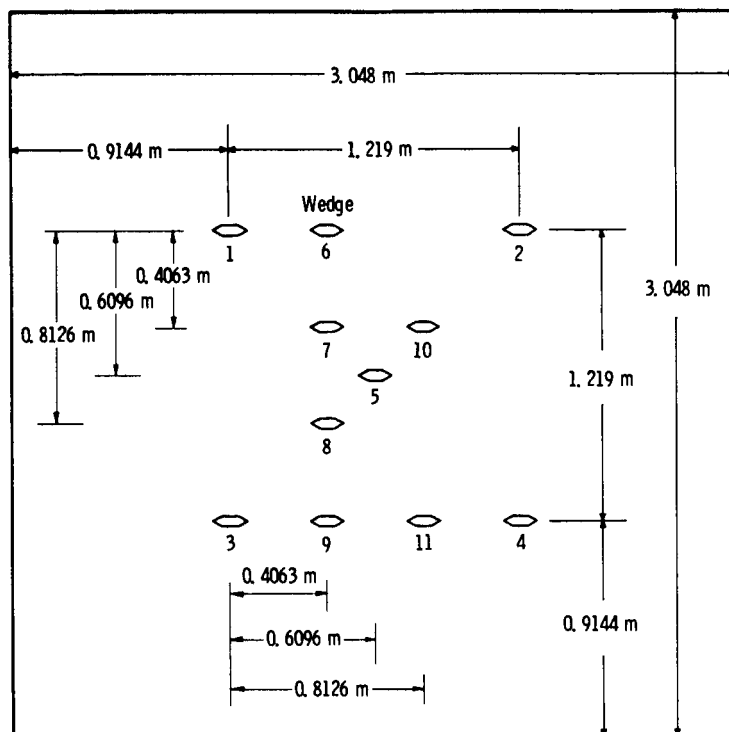
(a) Wedge arrangement in test section.
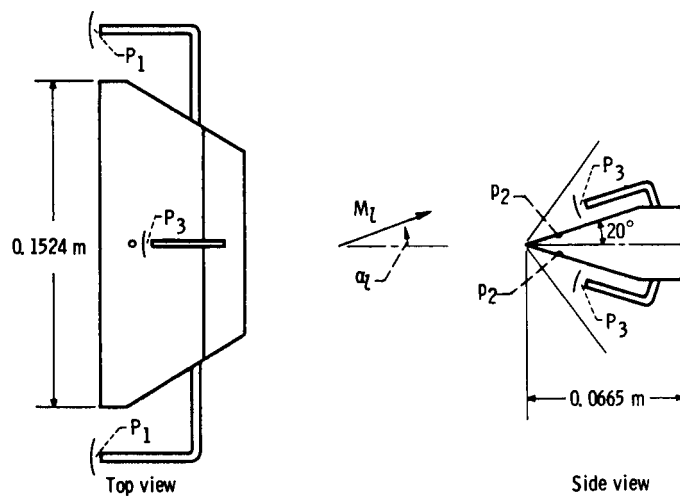
(b) Details of steady-state instrumentation and wedge design for survey rake wedges 1 to 9.

Figure 4. – Survey rake details.
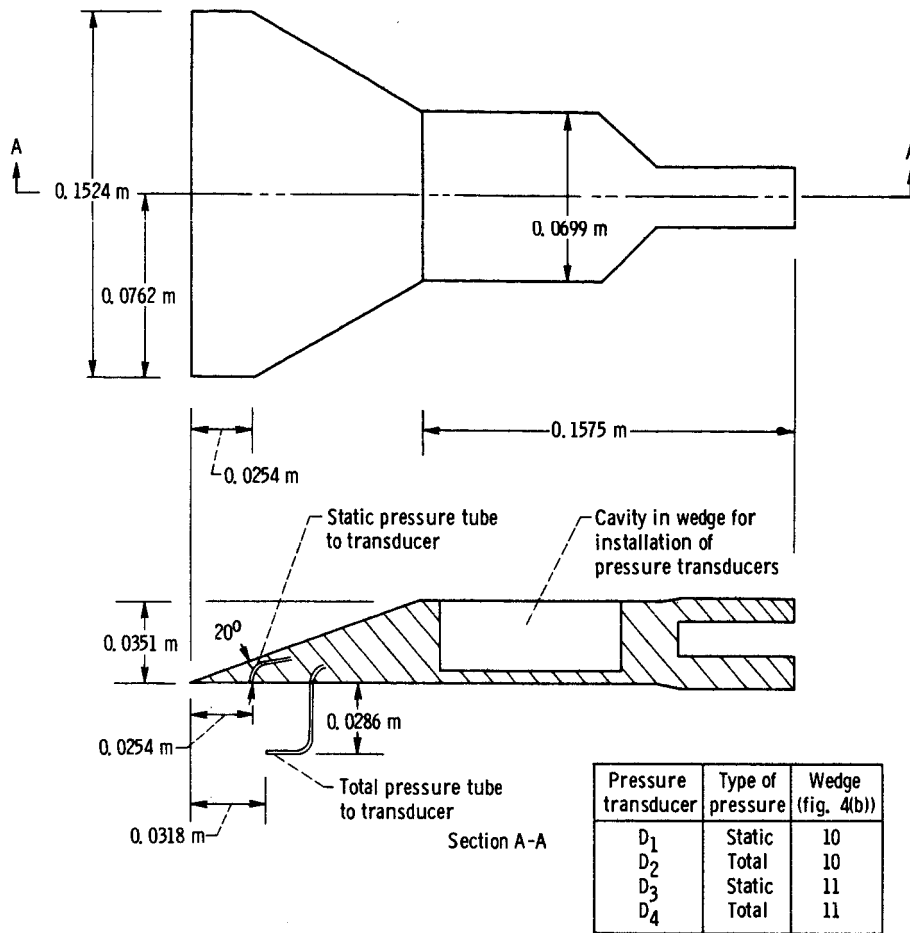
(c) Details of dynamic instrumentation and wedge design. Wedge number is shown. Wedge 11 was inverted.

Figure 4. - Concluded.

(a) Local Mach number.

(b) Local airflow angle.

(c) Local total pressure recovery.
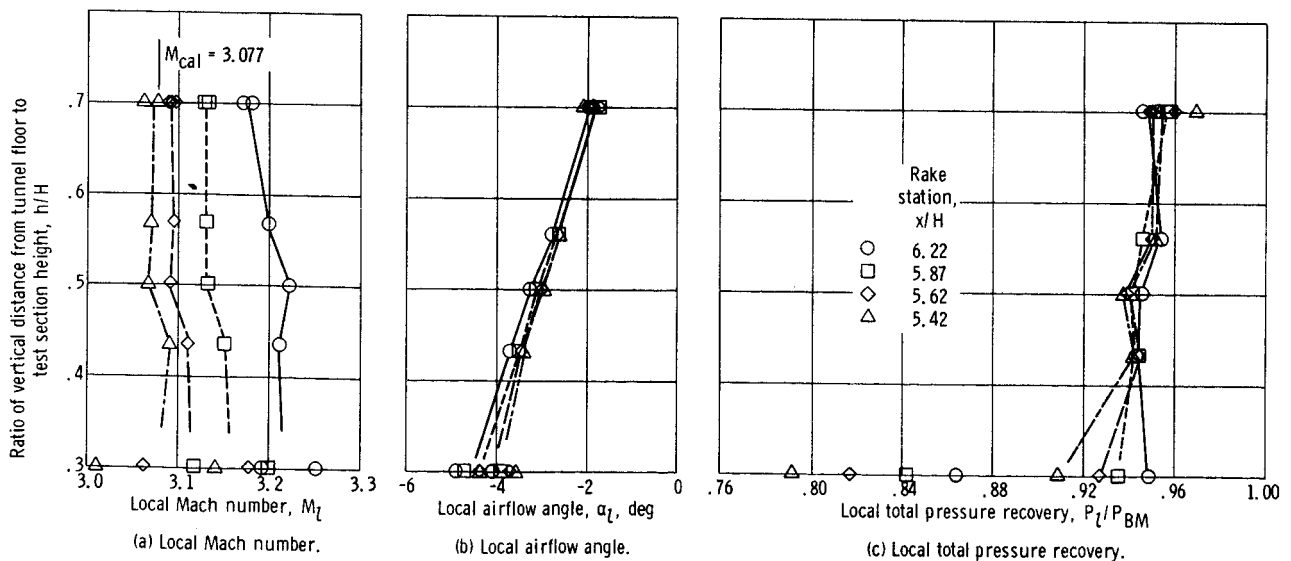
Figure 5. - Local test section conditions. Gust plate configuration LA3.1; wall Mach number, 3.1; Reynolds number, 8.37x10^6 per meter.
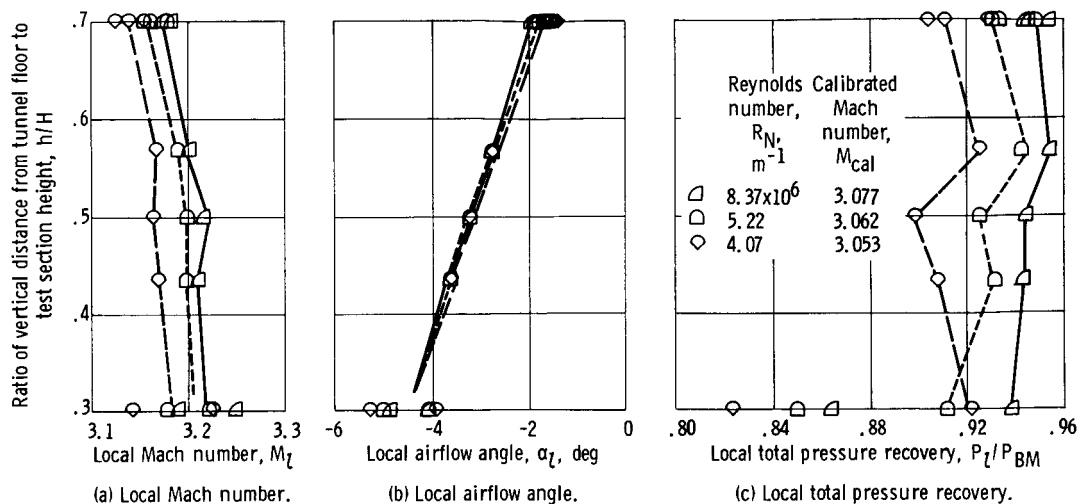
Figure 6. - Effect of Reynolds number on local test section conditions at rake station x/H of 6.22 for gust plate configuration LA3.1. Wall Mach number, 3.1.
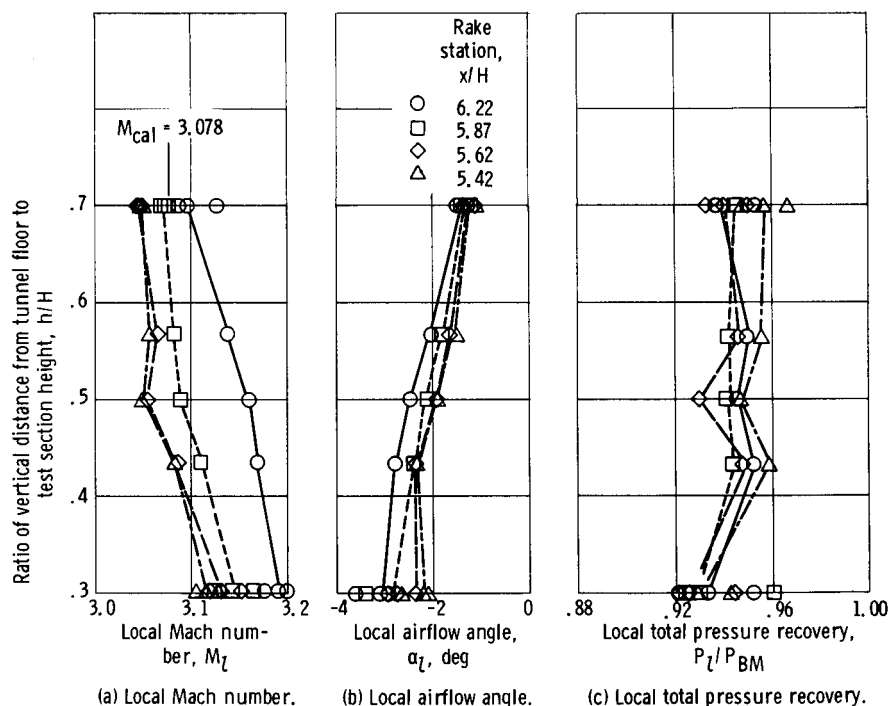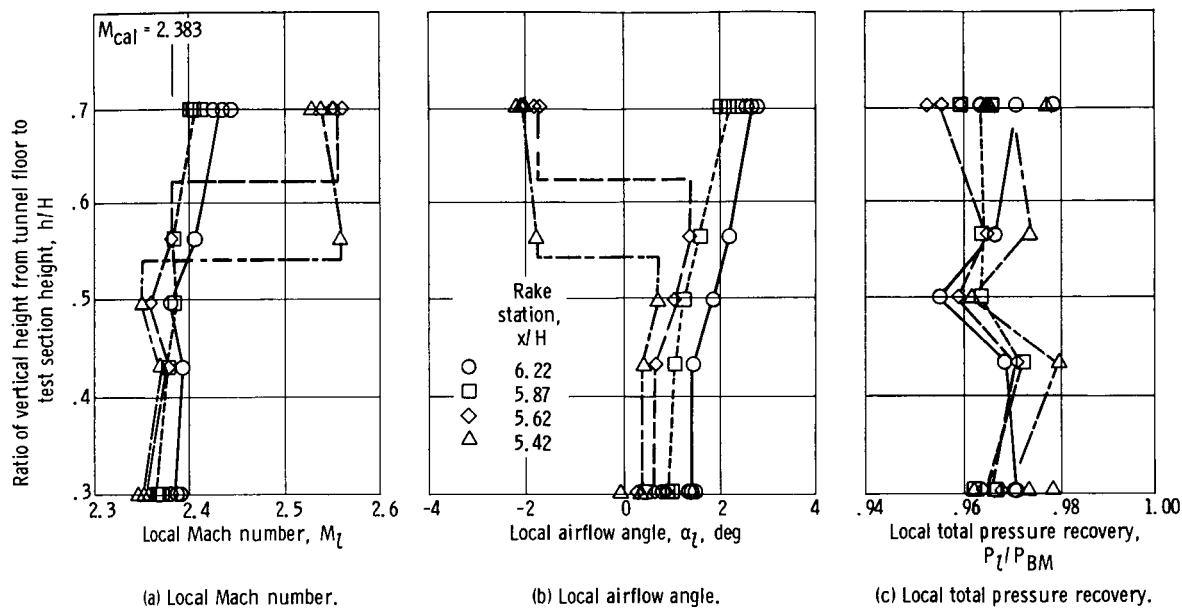

Figure 7. - Local test section conditions. Gust plate configuration SZ3.1; wall Mach number, 3.1; Reynolds number, 8.63x10^{6} per meter.
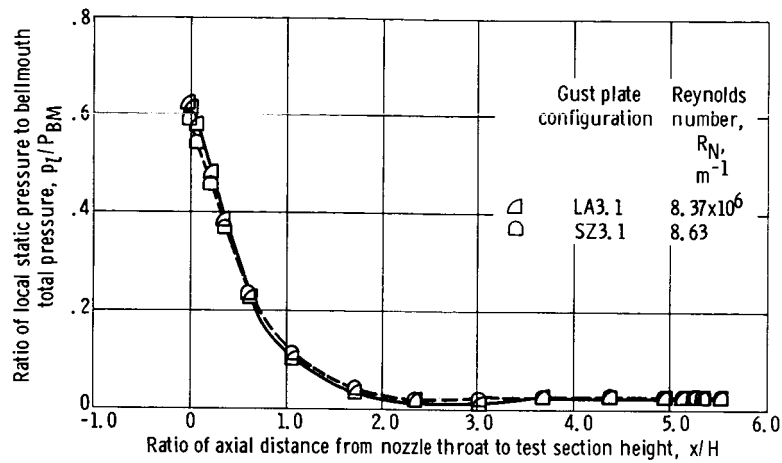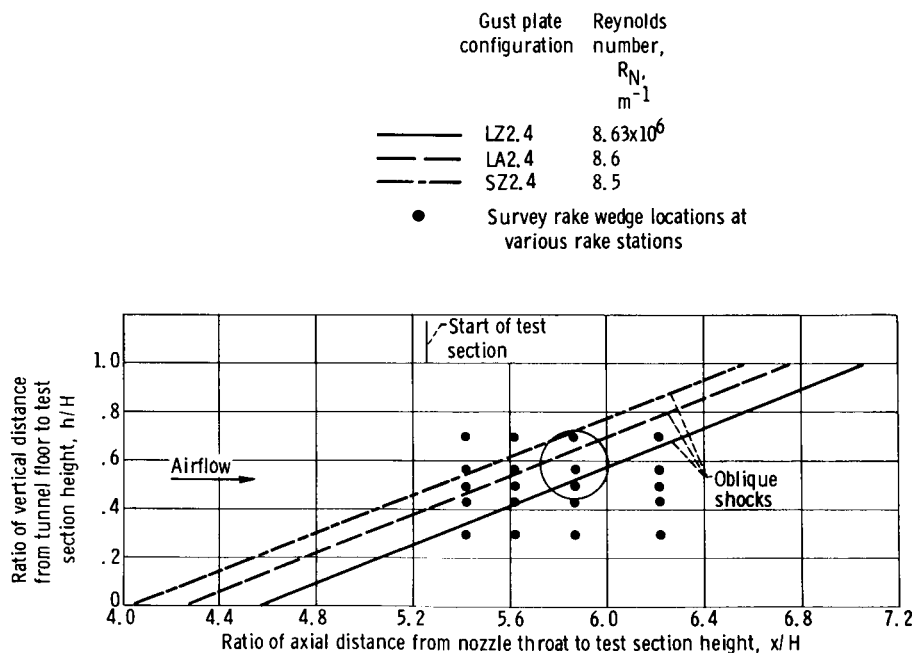
Figure 8. – Nozzle and test section ceiling centerline static pressure distributions. Wall Mach number, 3.1.

(a) Local Mach number.

(b) Local total pressure recovery.
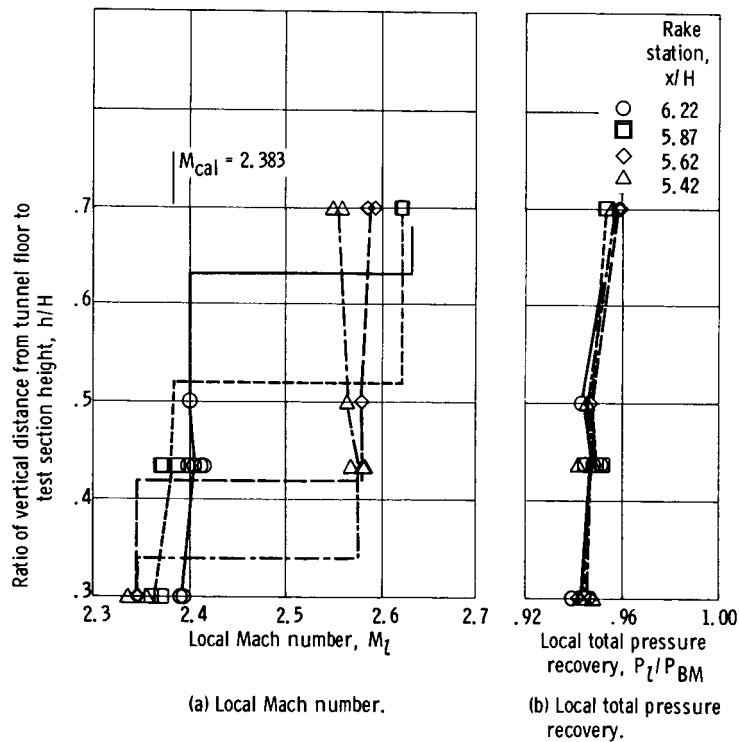
Figure 9. – Local test section conditions. Gust plate configuration LZ2.4; wall Mach number, 2.4; Reynolds number, 8.63x10^6 per meter; rake rotated 90°.

Figure 11. - Effect of Reynolds number on local test section Mach number at rake station x/H of 5.42 for gust plate configuration LZ2.4. Wall Mach number, 2.4.

Local Mach number, M_l

Ratio of vertical distance from tunnel floor to test section height, h/H

Reynolds number, R_N, m^{-1}	Calibrated Mach number, M_{cal}
8.63x10^6	2.383
5.24	2.365

Airflow
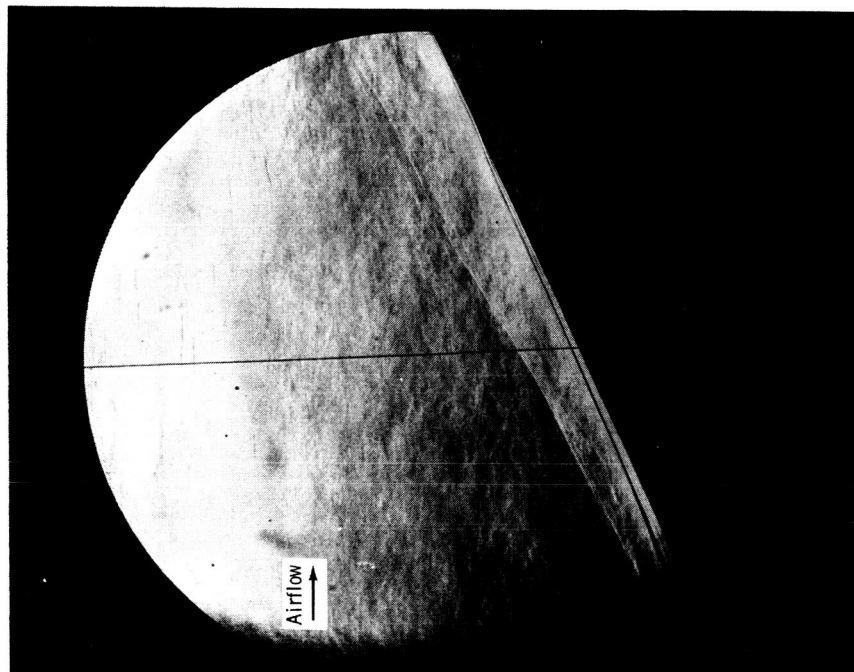
Figure 10. - Schlieren photograph of oblique shock wave. Gust plate configuration LZ2.4; wall Mach number, 2.4; Reynolds number, 8.63x10^6 per meter.
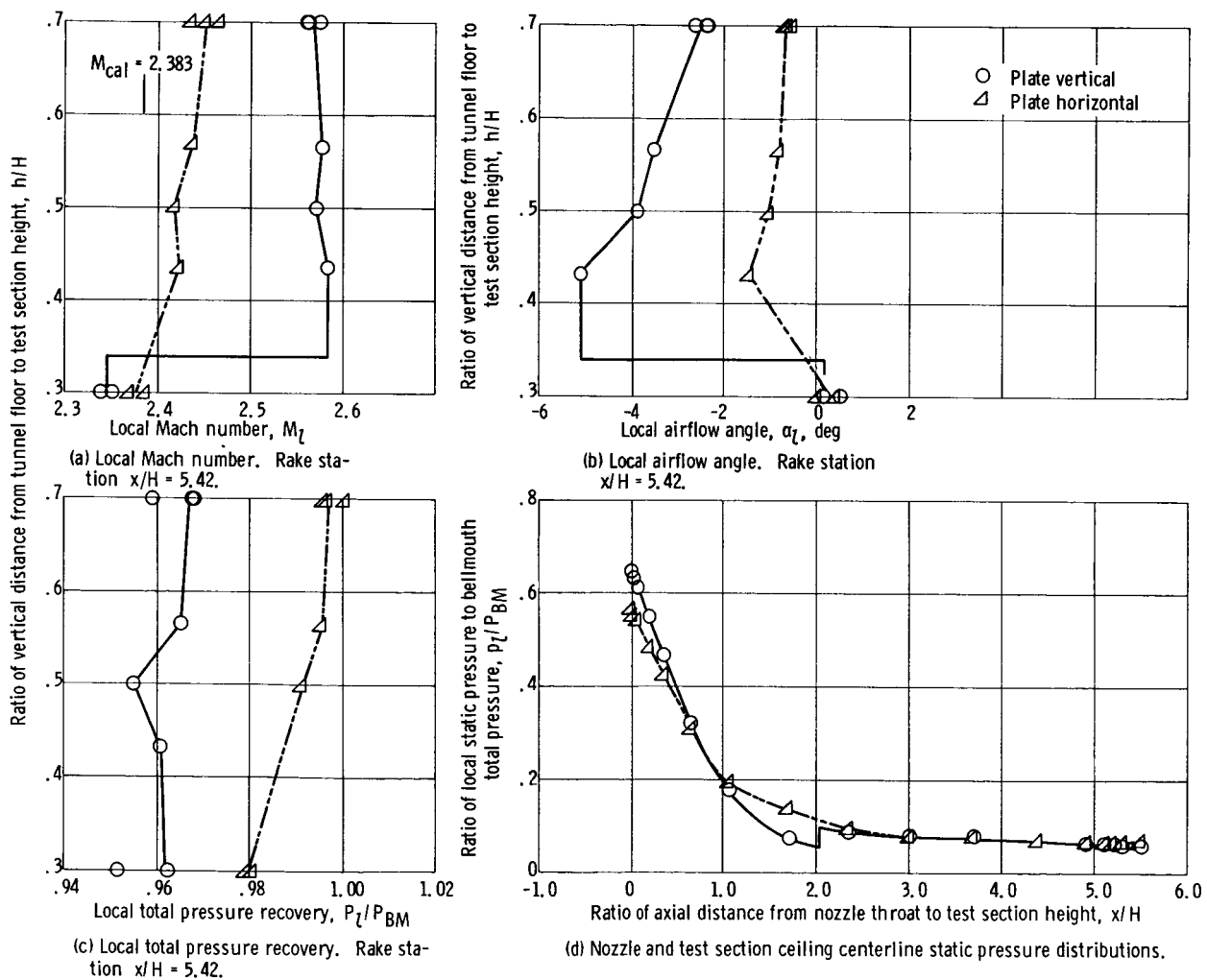
(a) Local Mach number. (b) Local airflow angle. (c) Local total pressure recovery.
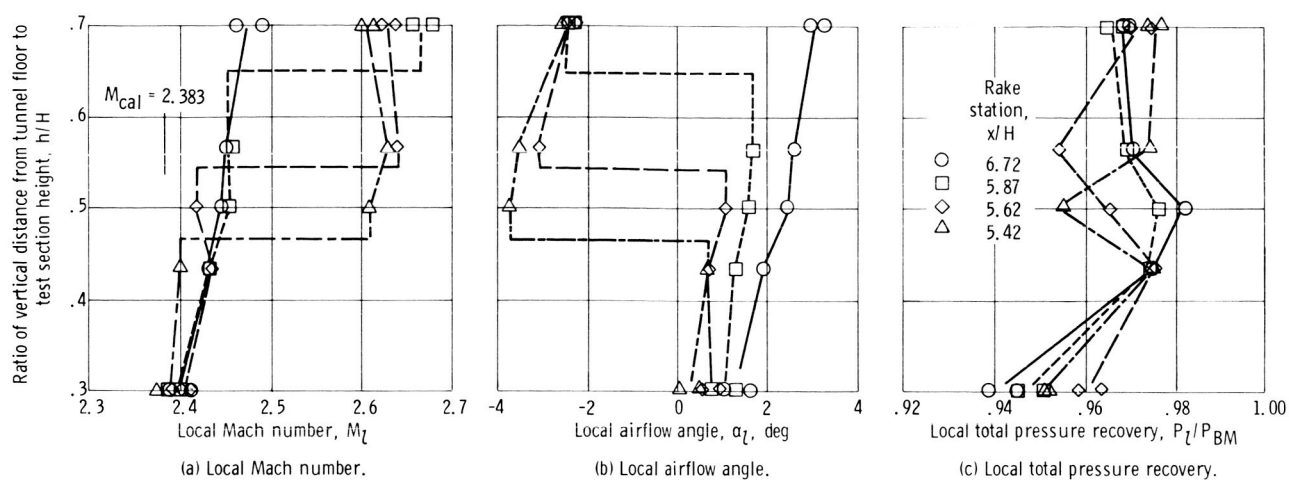
Figure 12. - Local test section conditions. Gust plate configuration LA2.4; wall Mach number, 2.4; Reynolds number, 8.6×10^6 per meter.
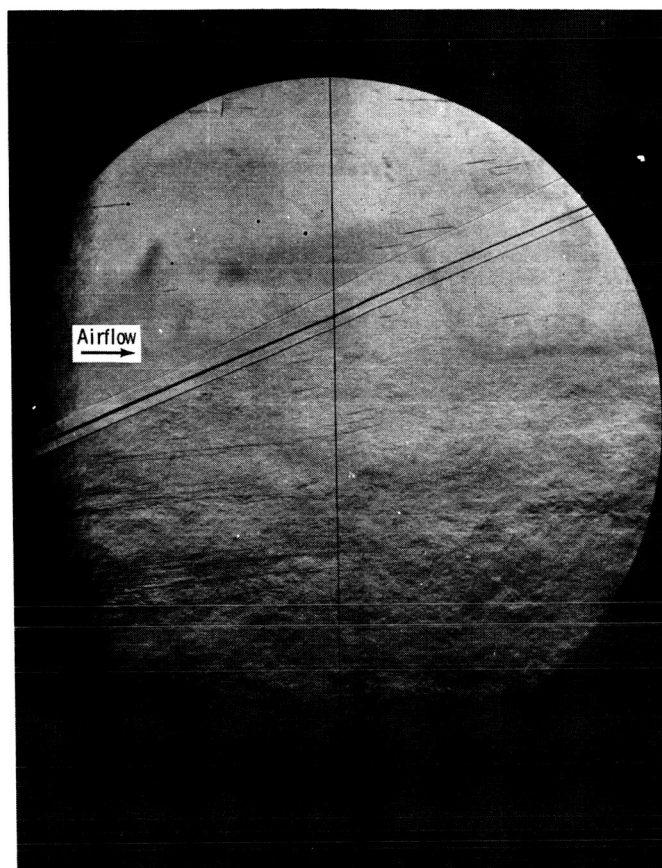
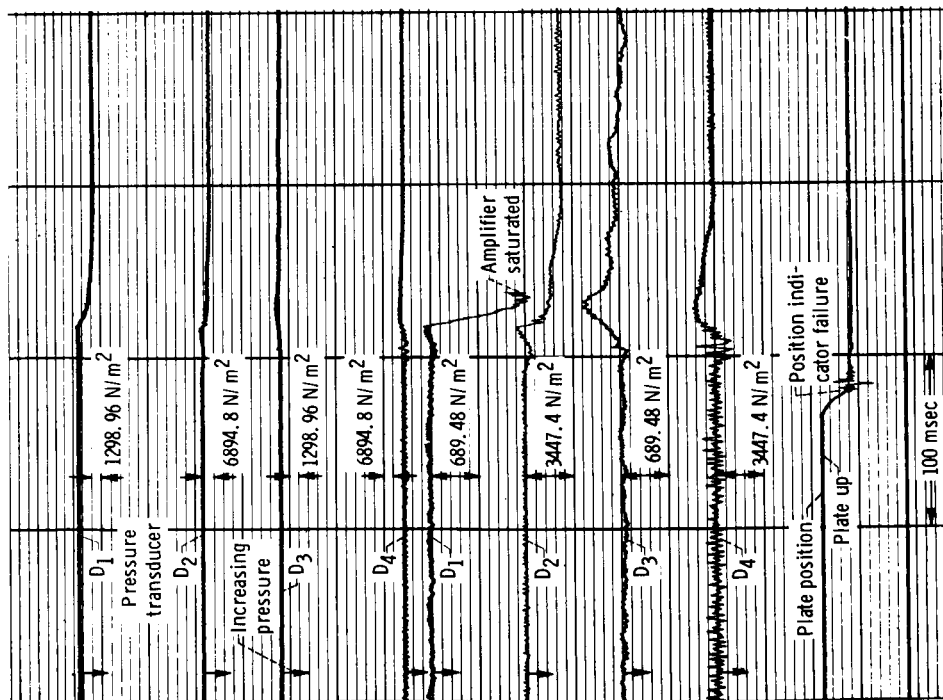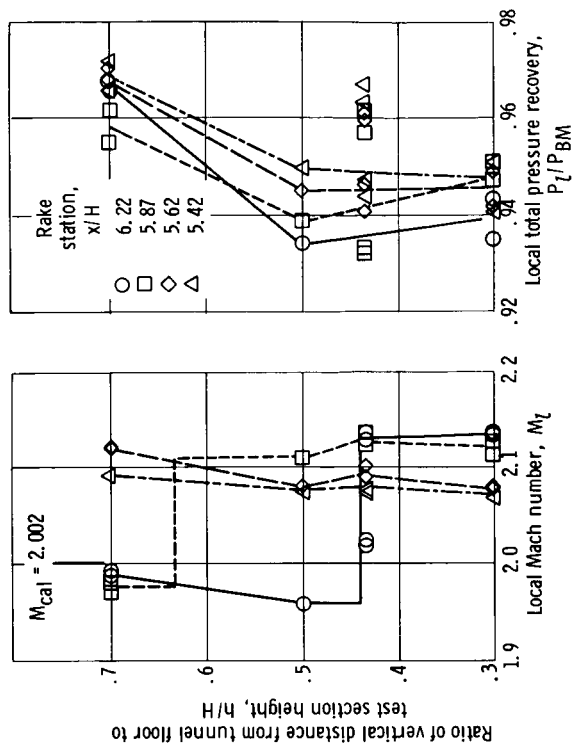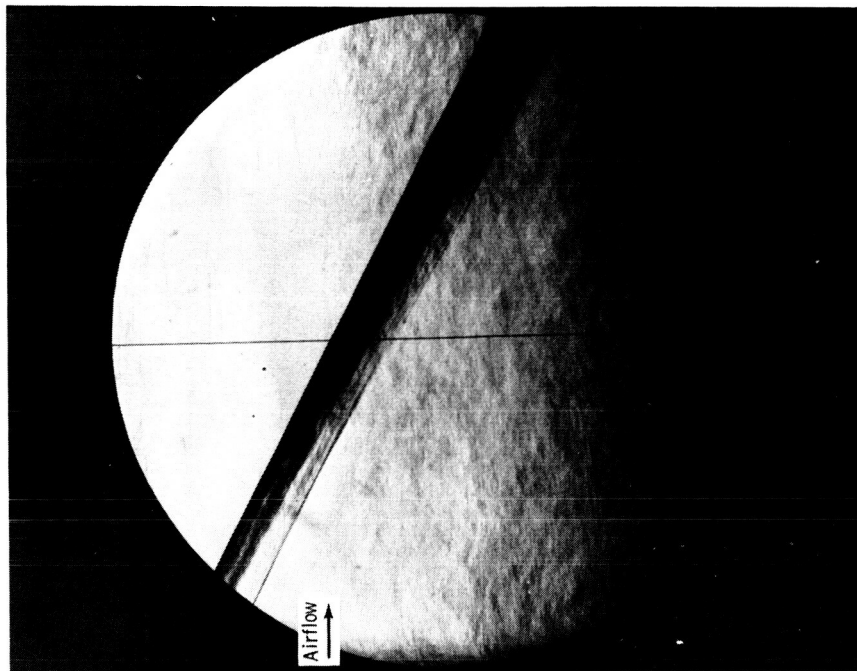Figure 13. - Schlieren photograph of oblique shock wave. Gust plate configuration LA2.4; wall Mach number, 2.4; Reynolds number, 8.6×10^6 per meter.

(a) Local Mach number.

(b) Local airflow angle.

(c) Local total pressure recovery.

Figure 14. - Local test section conditions. Gust plate configuration SZ2.4; wall Mach number, 2.4; Reynolds number, 8.5x10^{6} per meter.

Figure 15. - Sketch of part of nozzle and test section which shows locations of oblique shock waves that were obtained at wall Mach number of 2.4 for different gust plates.
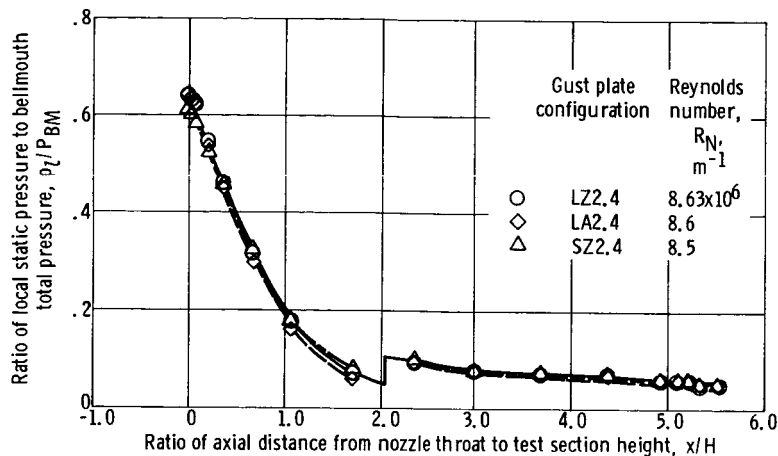
Figure 16. - Nozzle and test section ceiling centerline static pressure distributions. Wall Mach number, 2.4.

(a) Local Mach number. Rake station x/H = 5.42.

(b) Local airflow angle. Rake station x/H = 5.42.

(c) Local total pressure recovery. Rake station x/H = 5.42.

(d) Nozzle and test section ceiling centerline static pressure distributions.

Figure 17. - Local test section conditions before and after rotation of gust plate configuration LZ2.4. Wall Mach number, 2.4; Reynolds number, 8.56x10⁶ per meter.

Figure 19. - Local test section conditions. Gust plate configuration LZ2.4; wall Mach number, 2.0; Reynolds number, 8.56×10^6 per meter; rake rotated 90^0.

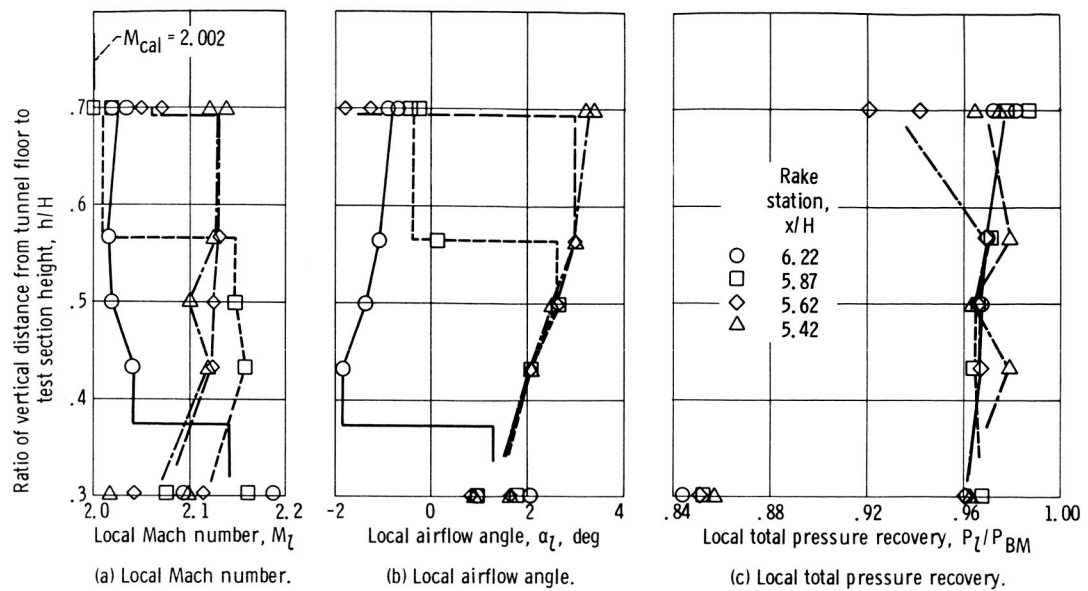(a) Local Mach number.

(b) Local total pressure recovery.

Figure 18. - Transient recording of plate position and wedge 10 and 11 pressures obtained during airflow gust created by rotation of gust plate LZ2.4.
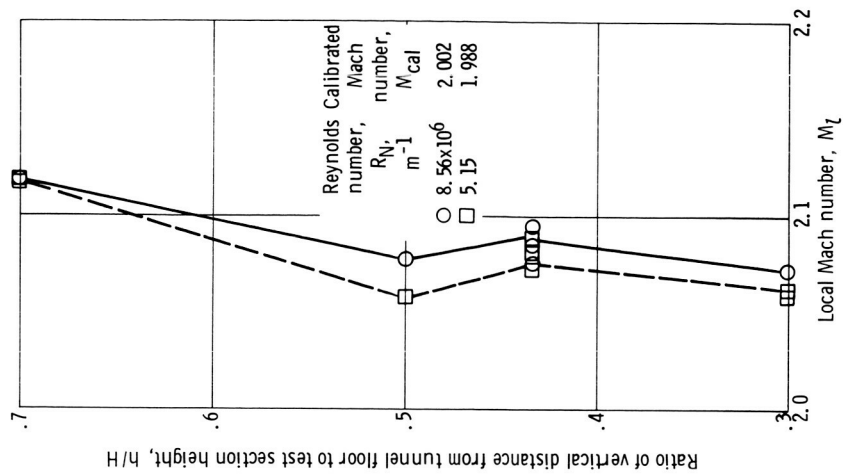
Figure 21. - Effect of Reynolds number on local test section Mach number at rake station x/H of 5.42 for gust plate configuration LZ2.4. Wall Mach number, 2.0.
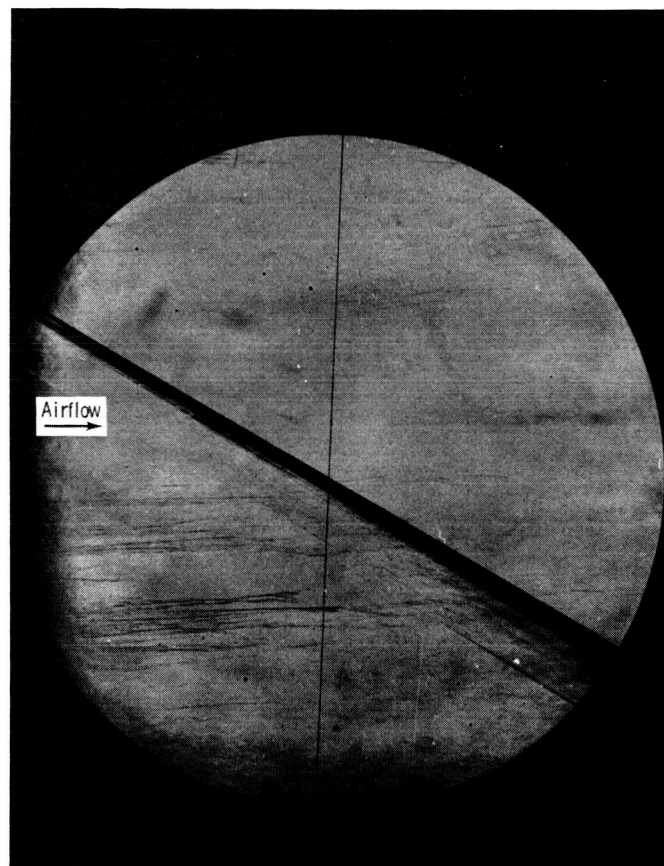

Figure 20. - Schlieren photograph of oblique shock wave. Gust plate configuration LZ2.4; wall Mach number, 2.0; Reynolds number 8.56x10⁶ per meter.

(a) Local Mach number. (b) Local airflow angle. (c) Local total pressure recovery.

Figure 22. - Local test section conditions. Gust plate configuration LA2.4; wall Mach number, 2.0; Reynolds number, 8.46x10^{6} per meter.

(a) Reynolds number, 8.46x10^{6} per meter.

Figure 23. - Schlieren photographs of oblique shock wave. Gust plate configuration LA2.4; wall Mach number, 2.0.
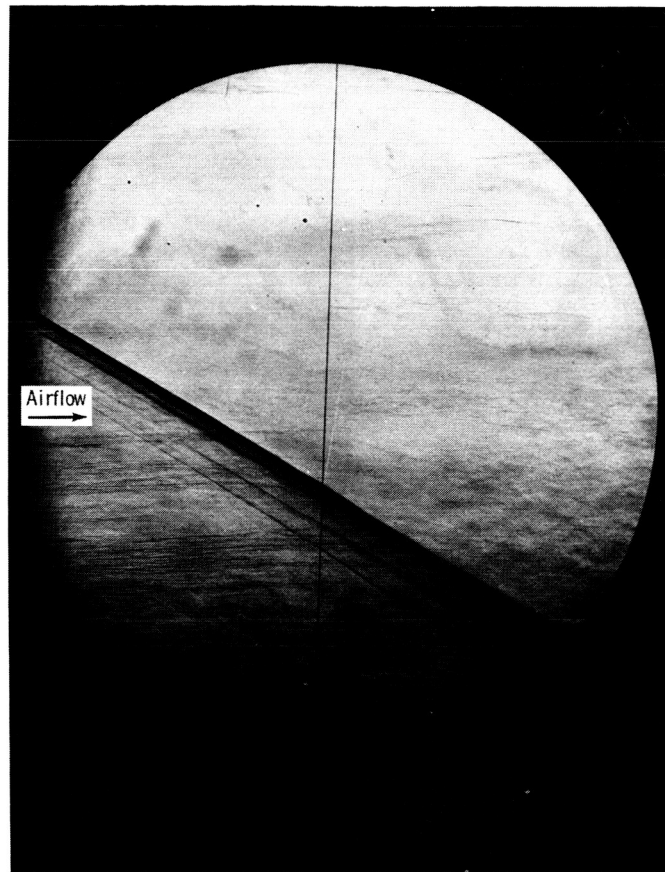
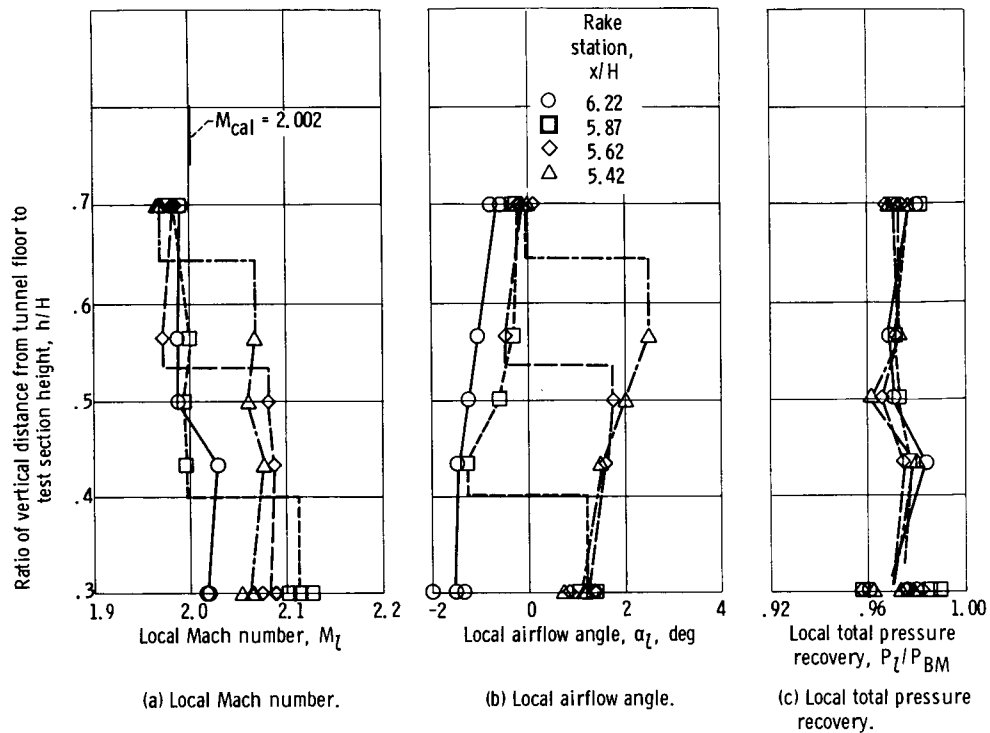(b) Reynolds number, 5.18×10^6 per meter.

Figure 23. - Concluded.

(a) Local Mach number. (b) Local airflow angle. (c) Local total pressure recovery.

Figure 24. – Local test section conditions. Gust plate configuration, SZ2.4; wall Mach number, 2.0; Reynolds number, 8.46×10^6 per meter.
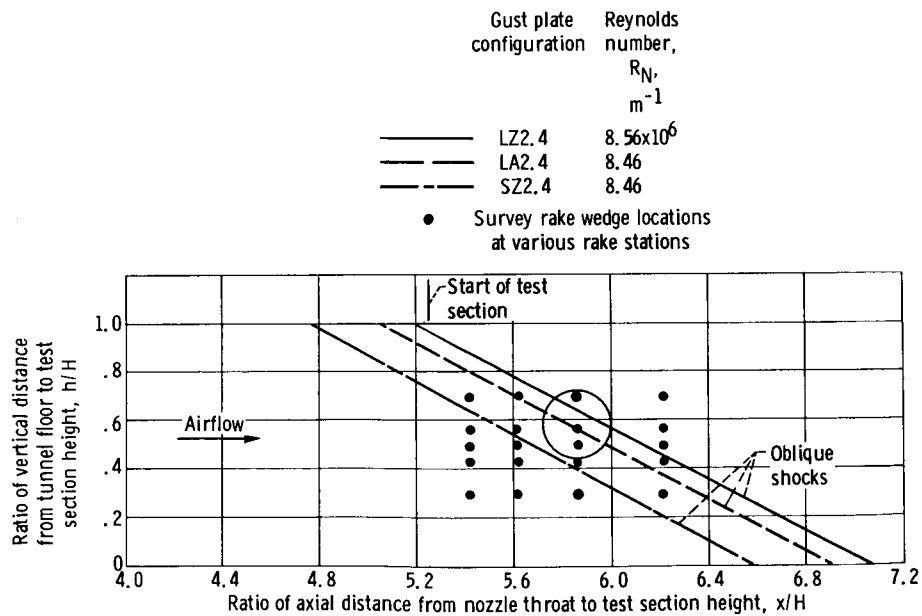

Figure 25. – Sketch of part of nozzle and test section which shows locations of oblique shock waves that were obtained at wall Mach number of 2.0 for different gust plates.
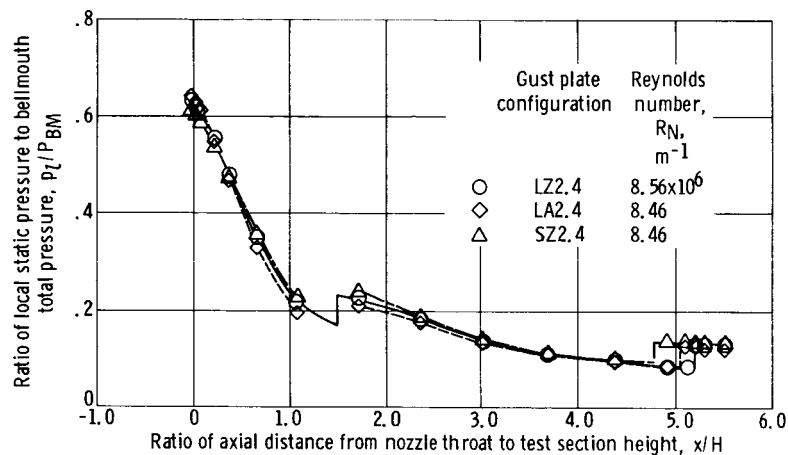
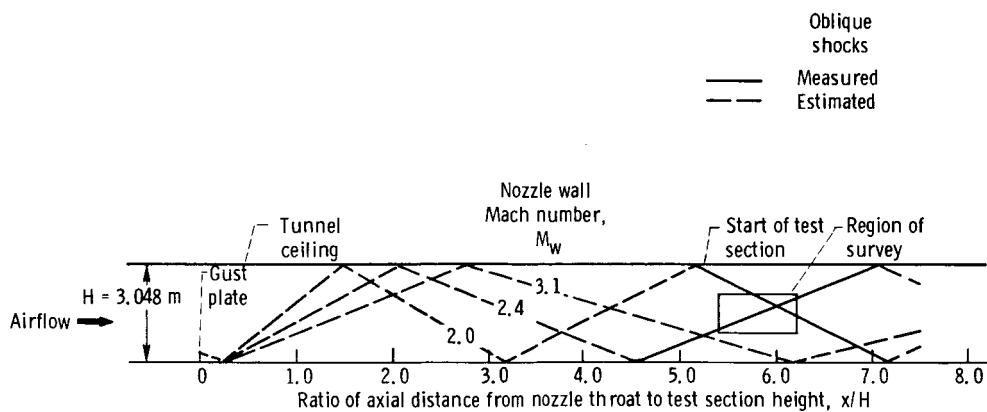Figure 26. - Nozzle and test section ceiling centerline static pressure distributions. Wall Mach number, 2.0.

Figure 27. - Typical oblique shocks for gust plate mounted on nozzle floor for nozzle wall Mach numbers of 2.0, 2.4, and 3.1.

1. Report No. NASA TM X-3120	2. Government Accession No.	3. Recipient's Catalog No.
4. Title and Subtitle GUST GENERATOR FOR A SUPERSONIC WIND TUNNEL		5. Report Date December 1974
		6. Performing Organization Code
7. Author(s) Bobby W. Sanders, Allan R. Bishop, and John A. Webb, Jr.		8. Performing Organization Report No. E-7978
		10. Work Unit No. 401-24
9. Performing Organization Name and Address Lewis Research Center National Aeronautics and Space Administration Cleveland, Ohio 44135		11. Contract or Grant No.
		13. Type of Report and Period Covered Technical Memorandum
12. Sponsoring Agency Name and Address National Aeronautics and Space Administration Washington, D.C. 20546		14. Sponsoring Agency Code

15. Supplementary Notes

16. Abstract

An investigation was conducted to determine the effectiveness of a flat plate gust generator that was located in the nozzle throat of the Lewis 10- by 10-Foot Supersonic Wind Tunnel. Gust plates were tested at nozzle wall Mach numbers of 3.1, 2.4, and 2.0. Test results indicate that the flat plate concept may be used as a gust generator for a wind tunnel; however, more extensive investigation is required to completely define its capabilities and limitations. For the single transient data point recorded, a gust amplitude (decrement) of 0.15 in Mach number was obtained. Analysis of these transient data indicated a response with a corner frequency of at least 8 hertz.

17. Key Words (Suggested by Author(s)) Wind tunnels Supersonic wind tunnels Gust generator	18. Distribution Statement Unclassified – unlimited STAR category 01		
19. Security Classif. (of this report) Unclassified	20. Security Classif. (of this page) Unclassified	21. No. of Pages 36	22. Price* $3.75